PAK–PIX interactions regulate adhesion dynamics and membrane protrusion to control neurite outgrowth

Miguel Santiago-Medina, Kelly A. Gregus and Timothy M. Gomez*

Department of Neuroscience, Neuroscience Training Program, University of Wisconsin, Madison, WI 53706, USA

*Author for correspondence (tmgomez@wisc.edu)

Accepted 26 November 2012
Journal of Cell Science 126, 1122–1133

doi: 10.1242/jcs.112607

Summary

The roles of P21-activated kinase (PAK) in the regulation of axon outgrowth downstream of extracellular matrix (ECM) proteins are poorly understood. Here we show that PAK1–3 and PIX are expressed in the developing spinal cord and differentially localize to point contacts and filopodial tips within motile growth cones. Using a specific interfering peptide called PAK18, we found that axon outgrowth is robustly stimulated on laminin by partial inhibition of PAK–PIX interactions and PAK function, whereas complete inhibition of PAK function stalls axon outgrowth. Furthermore, modest inhibition of PAK–PIX stimulates the assembly and turnover of growth cone point contacts, whereas strong inhibition over-stabilizes adhesions. Point mutations within PAK confirm the importance of PIX binding. Together our data suggest that regulation of PAK–PIX interactions in growth cones controls neurite outgrowth by influencing the activity of several important mediators of actin filament polymerization and retrograde flow, as well as integrin-dependent adhesion to laminin.

Key words: Axon guidance, Focal adhesion, Pathfinding, Neural development, Regeneration, Pak-interacting exchange factor

Introduction

During development, complex neuronal circuits assemble through guided extension of billions of axons to their correct synaptic target sites. Growth cones at the tips of developing axons use molecular guidance cues deposited in their immediate environment to guide axons to distant targets (Kolodkin and Tessier-Lavigne, 2011). Growth cones integrate signals generated through receptor interactions with ligands that both promote and inhibit axon outgrowth (Lowery and Van Vactor, 2009). Intracellular signals converge on the cytoskeleton, which powers the force-generating machinery that controls membrane protrusion and retraction (Dent et al., 2011).

Analogous to migrating cells, the regulation of growth cone motility requires the coordination of leading-edge membrane protrusion, adhesion, de-adhesion and retraction (Marín et al., 2010). Although many studies have focused on the molecular basis of filopodial and lamellipodial protrusion/retraction, far less is known about the signals that control adhesion/de-adhesion. The stabilization of new protrusions to the ECM occurs at specialized adhesion sites called point contacts (PCs), which are analogous to focal contacts (FCs) of most crawling cells. Growth cone PCs link integrin receptors to the actin cytoskeleton by recruiting various adaptor and signaling proteins (Myers et al., 2011; Santiago-Medina et al., 2011). By linking F-actin to the underlying substratum, PCs restrain myosin-based retrograde flow of F-actin to support membrane protrusion and forward growth cone translocation.

A number of structural proteins, such as the multi-domain scaffolding protein paxillin (PXN), link actin filaments to integrins. Moreover, FCs and PCs also contain a myriad of signaling proteins that modulate adhesion assembly and disassembly (adhesion dynamics) through phosphorylation (Zaidel-Bar and Geiger, 2010). For example, paxillin is phosphorylated at N-terminal tyrosine residues by protein tyrosine kinases and at serine residues by p21-activated kinase (PAK) (Deakin and Turner, 2008; Nayal et al., 2006). Phosphorylation of these sites in response to growth factors and guidance cues serves to regulate adhesion dynamics and coordinate additional downstream signals. Recent evidence suggests that the assembly, distribution and dynamic turnover of growth cone PCs is a fundamental regulator of axon outgrowth and guidance (Carlstrom et al., 2011; Hines et al., 2010; Marsick et al., 2012; Myers and Gomez, 2011).

PAK proteins are a conserved family of serine/threonine kinases involved in signaling pathways downstream of the Rho family GTPases, Rac1 and Cdc42 (Bokoch, 2003). PAK1–3 (Group 1) consist of an N-terminal regulatory domain and a C-terminal kinase domain. The N-terminal regulatory domain contains an activating p21 GTPase-binding domain (PBD), as well as an auto-inhibitory domain (AID) (Arias-Romero and Chernoff, 2008). Adjacent to the PBD/AID domain is a proline-rich motif that interacts with the guanine nucleotide exchange factor (GEF), PIX (Manser et al., 1998). PAK has been shown to target FCs through PIX, which links to paxillin through paxillin kinase linker (PKL; also known as GIT2) (Brown et al., 2002; Turner et al., 1999). Therefore, this GIT–PIX–PAK complex may target Rac1 and its effector PAK to adhesion sites (ten Klooster et al., 2006). The binding of this complex to paxillin is regulated by PAK-dependent phosphorylation of S273 of paxillin, which could increase local Rac1 activity (Deakin and Turner, 2008; Nayal et al., 2006; ten Klooster et al., 2006). However, PAK–PIX interactions can also mediate functions independently of activating Rho GTPases.

In non-neuronal cells, PAK controls cell motility by regulating the organization and dynamic assembly of actin filaments,

Journal of Cell Science

microtubules and substratum adhesions (Bokoch, 2003). In neurons, different PAK isoforms have been shown to regulate various aspects of neuronal development, such as neuronal cell fate, migration, polarization and neurite initiation and guidance (Cobos et al., 2007; Daniels et al., 1998; Hayashi et al., 2002; Kreis and Barnier, 2009). We previously demonstrated that at least one isoform of PAK localizes to the tips of extending filopodia in an Src-kinase-dependent manner (Robles et al., 2005). PAK disfunction has also been implicated in neurodegenerative diseases and neuronal development disorders, such as X-linked mental retardation (Kreis and Barnier, 2009; Zhang et al., 2005). Despite a clear role for PAK neuronal development, almost nothing is known about how PAK controls growth cone motility. Understanding how the spatial and temporal activity of distinct PAK isoforms influences growth cone adhesion and motility downstream of axon guidance cues is crucial to understanding neural development.

In this study, we show that PAK1–3 are expressed in spinal neurons and that PAK2 and 3 localize to distinct sub-cellular regions within growth cones. xPAK2 localizes to growing filopodial tips, as well as to paxillin-containing adhesions, whereas xPAK3 only localizes to adhesions. We also find that α-PIX localizes with PAK to paxillin-containing adhesions. Inhibition of PAK–PIX interactions with PAK18 results in dose-dependent effects on neurite outgrowth and growth cone morphology through its downstream actin effectors ADF/cofilin and myosin-II. Moreover, PAK regulates integrin-based adhesion dynamics to further influence axonal outgrowth. Taken together, our findings suggest that PAK functions on two main determinants of growth cone motility, the actin cytoskeleton and adhesive point contacts, to regulate axon outgrowth on ECM proteins.

Results

PAK is expressed in the developing spinal cord and localizes to growth cone point contacts and filopodia tips

Most vertebrates, including *Xenopus laevis*, express six PAK proteins from distinct genes. PAK proteins are divided into two groups, based upon sequence and structural homology: group I (PAK1–3) and group II (PAK4–6) (Bisson et al., 2003; Bowes et al., 2010; Cau et al., 2000; Souopgui et al., 2002). Group I PAK proteins are most highly expressed in developing neurons, suggesting important roles in neuronal differentiation and function in early development (Kreis and Barnier, 2009). To begin to study the function of PAK in the control of growth cone motility, we determined the expression pattern of group I PAK transcripts in the developing *Xenopus* spinal cord. Using *Xenopus laevis* specific primers, we amplified PAK1–3 transcripts by RT-PCR from mRNA isolated from pure stage 24 *Xenopus* spinal cord, suggesting all three members are expressed in spinal neurons (Fig. 1A). We also found that transcripts for the PAK-binding partners α- and β-PIX were present in spinal cord tissue. Although all three PAK isoforms were present, PAK2 and PAK3 transcripts appeared most abundant, consistent with *in situ* hybridizations of spinal cord of a similar developmental age (Souopgui et al., 2002). Using isoform-specific PAK antibodies, we immunoblotted for PAK1, 2 and 3 proteins from stage 24 pure spinal cord preparations. Consistent with our PCR results, we found that PAK2 and PAK3 proteins are highly expressed in the spinal cord, but PAK1 was not detected at the expected molecular mass (Fig. 1B) using two different PAK1 antibodies. These

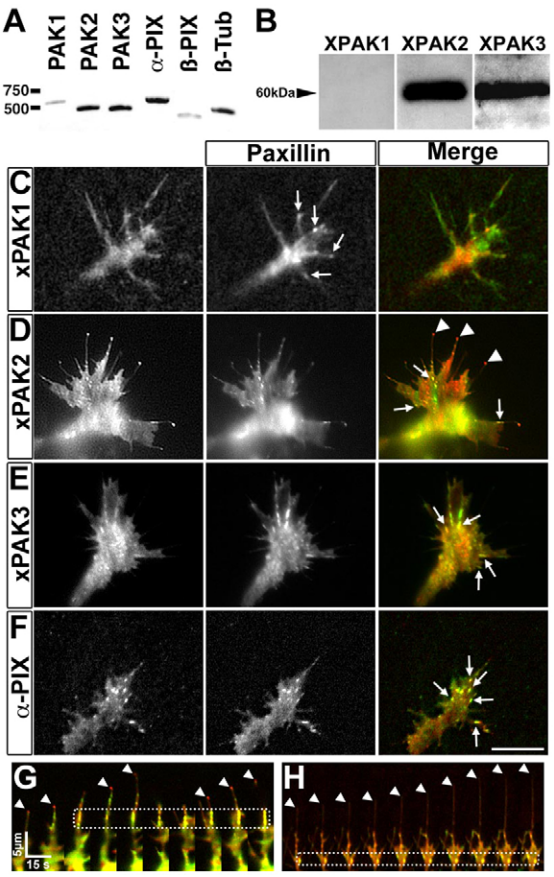

Fig. 1. PAK and PIX isoforms are expressed in the embryonic spinal cord and fusion proteins localize to distinct sites within live growth cones. (**A**) RT-PCR amplification of PAK1, 2, 3 and α-, β-PIX from stage 24 *Xenopus* spinal cord shows that PAK2 and PAK3, as well as α-PIX are most highly expressed. (**B**) Western blot of PAK1, 2 and 3 from stage 24 *Xenopus* spinal cord confirms that PAK2 and PAK3 are highly expressed. (**C–F**) TIRF images of representative live spinal neuron growth cones on LN expressing PXN–GFP or PXN–mCh together with different isoforms of fluorescent PAK (C–E) or α-PIX (F). (C) xPAK1 does not concentrate at any distinct location within this growth cone and does not colocalize with PXN-containing point contacts (PCs). (D) xPAK2 localizes to PXN-containing PCs (arrows) and to filopodial tips that contain little or no PXN (arrowheads). (E) xPAK3 localizes to only PXN-containing PCs (arrows). (F) α-PIX localizes to only PXN-containing PCs (arrows). (**G**,**H**) Montages of merged images of the growth cones shown in D and E, respectively, expressing mCh–xPAK2 and PXN–GFP (G) or mCh–xPAK3 and PXN–GFP (H); images were taken at 15 second intervals. Note in G that xPAK2 is present at the tips of extending filopodia (arrowheads) and colocalizes with PXN at stable point contacts (dashed box). In H xPAK3 is not present in the filopodia tips (arrowheads), but does colocalize with PXN at stable point contacts (dashed box). Scale bar: 10 μm.

results suggest that PAK2 and PAK3 are the most prominent isoforms of PAK in the developing *Xenopus* spinal cord.

Previously we showed that dsRed–human PAK1 localizes to extending filopodial tips of growth cones cultured on poly-D-lysine (PDL) (Robles et al., 2005) and to both filopodial tips and PCs within growth cones cultured on laminin (LN; unpublished observations). As the subcellular localization of PAK family members may provide clues to isoform-specific functions, we examined the dynamic localization of GFP–xPAK1–3 (*Xenopus* PAKs) in developing spinal neurons on LN by total internal

reflection fluorescence (TIRF) microscopy. Neurons were double-labeled for individual GFP–xPAK isoforms together with paxillin–mCherry (PXN–mCh), to identify PCs. Unlike human PAK1, we found that GFP–xPAK1 was only cytosolic within migrating growth cones (Fig. 1C). In contrast, GFP–xPAK2 robustly targets both PCs and the tips of extending filopodia (Fig. 1D,G). Differences in the distribution of human versus *Xenopus* PAK isoforms may be due to sequence differences between species (Bisson et al., 2003). Interestingly, in contrast to xPAK1 and 2, GFP–xPAK3 was present exclusively at growth cone PCs and did not localize to filopodial tips (Fig. 1E,H). As a direct binding partner of PAK, PIX should also localize to paxillin-containing adhesion sites. To test this we expressed GFP–α-PIX together with PXN–mCh. We found that GFP–α-PIX localized with PXN–mCh in growth cone adhesion sites but not at the tips of filopodia (Fig. 1F). Although we have no antibodies that work well by immunocytochemistry (ICC), from our combined western blot and live localization studies we can conclude that the distributions of endogenous PAK and PIX isoforms within motile growth cones are distinct.

To assess whether the distribution of PAK isoforms was similar in mammalian neurons and *Xenopus*, we immunolabeled PAK1–3 in developing mouse neurons (supplementary material Fig. S1). Dissociated neurons from mouse hippocampus (supplementary material Fig. S1A–C) and cortex (supplementary material Fig. S1D–F) were labeled with antibodies to specific PAK isoforms. Interestingly, we observe activated PAK1 (p-Thr423) at the growth cone filopodial tips (supplementary material Fig. S1A,D), whereas PAK2 was present at the leading edge of the lamellipodia (supplementary material Fig. S1B,E) and PAK3 at regions reminiscent of adhesion sites within growth cones (supplementary material Fig. S1C,F). However, it should be noted that without additional adhesion markers, it is difficult to determine with certainty which PAK isoforms localize to PCs.

Acute PAK inhibition has dose-dependent effects on growth cone motility and morphology

To begin to examine how PAK activity may influence growth cone motility, we used PAK18, a cell-permeable peptide inhibitor of PAK function (Maruta et al., 2002; Zhao et al., 2006). PAK18 is composed of the TAT internalization peptide sequence fused to 18 amino acids from the PIX-interacting motif of mouse PAK3. This peptide is believed to inhibit PAK function by disrupting PAK–PIX interactions (Maruta et al., 2002). The amino acid sequence of PAK18 is 72%, 89% and 94% identical to *Xenopus* PAK1–3, respectively, and all substitutions are with conserved amino acids in xPAK2 and xPAK3. First we tested the dose-dependent effects of PAK18 on axon outgrowth by time-lapse microscopy. Unexpectedly, a low concentration of PAK18 (1 μM) applied acutely to spinal neurons on LN strongly stimulated lamellipodial and filopodial protrusions (Fig. 2A,E,F; supplementary material Movie 1 and 2), leading to an immediate and robust expansion of growth cone area (Fig. 2G) and prolonged acceleration in the rate of neurite outgrowth (Fig. 2A,D). Both the area of lamellipodium expansion (Fig. 2G), as well as the total number and length of filopodia increase in the presence of 1 μM PAK18 (Fig. 2H; supplementary material Movie 2). In contrast, a reversed PAK18 control peptide (see Materials and Methods), had no effect on neurite outgrowth at any dose (supplementary material Fig. S2).

Higher concentrations of PAK18 (10–50 μM) also resulted in an immediate increase in growth cone area (Fig. 2B,C,G; supplementary material Movie 1), but these concentration only briefly enhanced outgrowth (Fig. 2D). Instead, after 5–10 minutes in 10–50 μM PAK18, axons typically stalled or retracted (Fig. 2C). This result suggests that a modest inhibition of PAK is optimal for outgrowth, whereas strong inhibition of PAK negatively regulates outgrowth. Although off-target effects of PAK18 are possible, our evidence (below) suggests that 1–50 μM PAK18 results in a dose-dependent inhibition of PAK

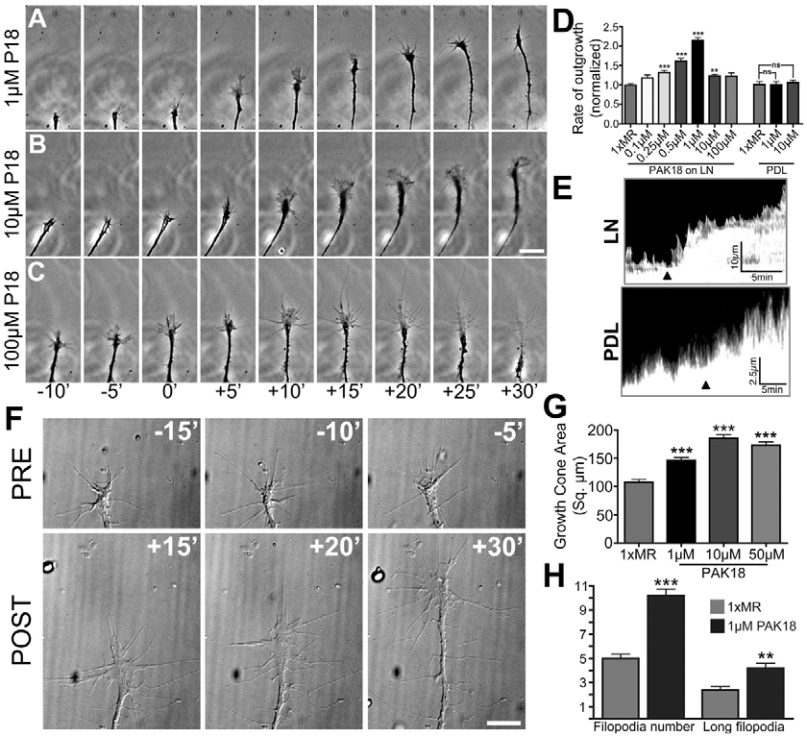

Fig. 2. Dose-dependent effects of acute inhibition of PAK–PIX interactions on growth cone motility and morphology. (**A–C**) Phase-contrast images at 5 minute intervals of growth cones on LN during stimulation with the indicated concentrations of PAK18 (at 0 minutes). (**D**) The rate of neurite outgrowth of neurons on LN and PDL after stimulation with increasing concentrations of PAK18 normalized to the pretreatment rate of outgrowth. Note that PAK18 maximally stimulates axon outgrowth on LN at 1 μM, but has no effect on neurite outgrowth on PDL at any concentration. Kruskal–Wallis test with Dunn's *post-hoc* analysis, $n \geq 60$. (**E**) Kymographs generated from the leading edge of fluorescent growth cones on LN (above) and PDL (below) during stimulation with 1 μM PAK18 (at black arrowhead). Note differences in scale bars. (**F**) DIC images of a growth cone on LN at 5 minute intervals during stimulation with 1 μM PAK18. Note an increase in growth cone area, as well as filopodia number and length after PAK18 stimulation. (**G**) Growth cone area was measured on fixed neurons after 5 minutes stimulation with different concentrations of PAK18. Kruskal–Wallis test with Dunn's *post-hoc* analysis, $n \geq 148$. (**H**) Number of filopodia and their length in response to 1 μM PAK18. The *y*-axis represents quantity. Student's *t*-test, $n \geq 27$. $^{**}P<0.01$, $^{***}P<0.001$. Scale bar: 20 μm (A–C) and 10 μm (F).

function. Notably, the rate of neurite outgrowth and growth cone area were inversely correlated, which is consistent with growth cone behavior seen *in vitro* and *in vivo* (Godement et al., 1994; Sretavan and Reichardt, 1993). Interestingly, axon extension was not stimulated by any concentration of PAK18 when neurons were cultured on the non-integrin binding substratum, PDL (Fig. 2D), although we did observe a slight increase in growth cone protrusion at 10 µM PAK18 (Fig. 2E). These results suggest that changes in integrin-dependent adhesion or signaling may contribute to enhanced growth cone motility on LN.

We also tested the effects of chronic PAK inhibition by culturing spinal neurons overnight in PAK18. After 16 hours in culture, spinal explants in control medium generated an average of 6.2±1.1 neurites per explant with an average length of 89.7±5.9 µm (supplementary material Fig. S3A,C,D). In contrast, spinal cord explants cultured in 1 µM PAK18 for 16 hours generated significantly more neurites per explant (24.8±1.9; $P<0.001$), which had a significantly longer average length (203.6±5.7 µm; $P<0.001$; supplementary material Fig. S3B–D). Additionally, neurons more often migrated away from explants when cultured in the presence of PAK18 (supplementary material Fig. S3B), suggesting that PAK18 also stimulates neuronal cell motility. Taken together, these results show that partial disruption of the PAK–PIX interaction with PAK18 promotes an immediate and sustained increase in neurite outgrowth.

PAK18 inhibits PAK-dependent targets to regulate actin polymerization and retrograde flow

PAK regulates a number of downstream targets known to modulate the cytoskeleton and influence cell membrane protrusion and motility (Bokoch, 2003). For example, PAK can regulate leading edge protrusions through actomyosin contractility or ADF/cofilin-mediated actin depolymerization. PAK can both increase [via direct phosphorylation of myosin light chain (MLC)] and decrease (by inhibition of MLC kinase) myosin-II driven actin contractility (Bokoch, 2003). In addition, active PAK reduces ADF/cofilin-mediated actin depolymerization by phosphorylating LIM kinase (LIMK). Active LIMK phosphorylates and inactivates ADF/cofilin to reduce its binding to F-actin, thus inhibiting actin severing. Therefore, PAK may control growth cone motility by regulating myosin-II driven F-actin contractility and ADF/cofilin-induced F-actin depolymerization.

To determine how disrupting PAK–PIX interactions modulates PAK targets, we first measured the levels of phosphorylated *Xenopus* ADF/cofilin (p-XAC) and myosin light-chain (p-MLC) in response to 1, 10 and 50 µM PAK18 by quantitative ICC (Fig. 3A–J). We measured the level of p-XAC (a direct target of LIMK) and p-MLC in growth cones after 5 minutes treatment with PAK18. We found that PAK18 reduces the levels of p-XAC in growth cones in a dose-dependent manner (Fig. 3A–E), further indicating that this peptide inhibits PAK function. To confirm that reduced p-XAC was not the result of increased growth cone

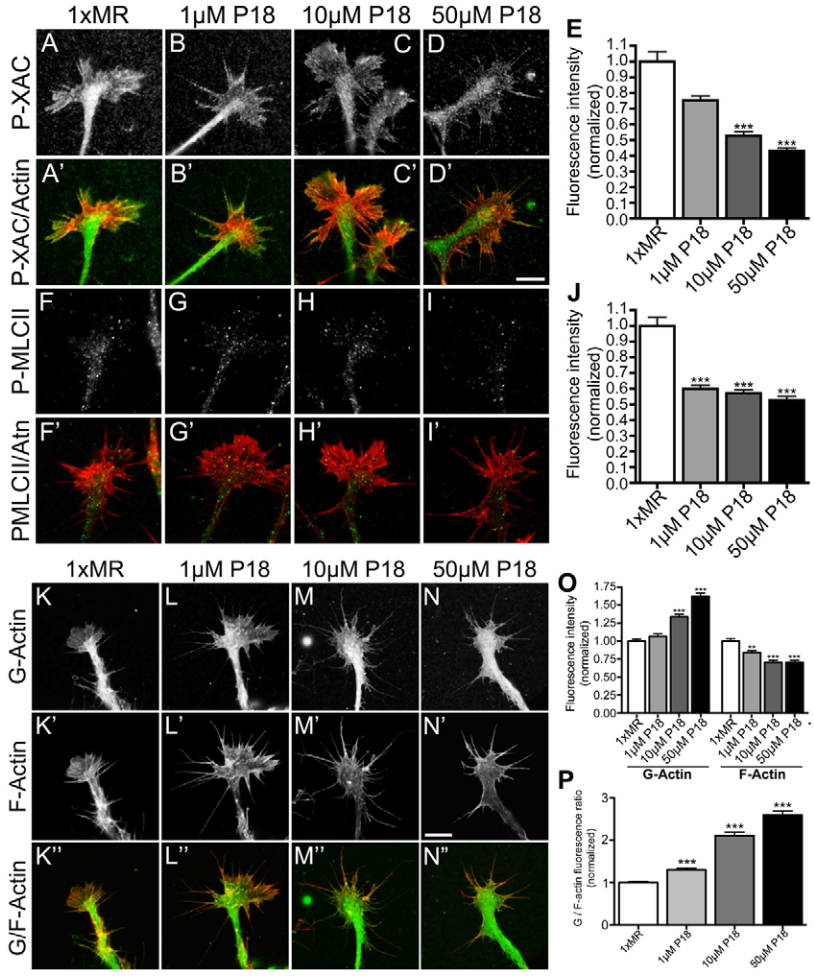

Fig. 3. Acute inhibition of PAK with PAK18 has dose-dependent effects on PAK targets and regulates actin polymerization. (**A–D**) Representative growth cones treated for 5 minutes with control medium or increasing concentrations of PAK18, and immunolabeled for p-XAC (Ser3). (**A′–D′**) Merged images of p-XAC (green) and F-actin labeling (red). (**E**) Fluorescence intensity measurements, normalized to control, of p-XAC labeling of growth cones treated with increasing concentrations of PAK18. (**F–I**). Representative growth cones treated for 5 minutes with control medium or increasing concentrations of PAK18 and immunolabeled for p-MLC. (**F′–I′**) Merged images of p-MLC (green) and F-actin labeling (red). (**J**) Normalized fluorescence intensity measurements of p-MLC-labeled growth cones. (**K–N**) Representative growth cones treated for 5 minutes with control medium or increasing concentrations of PAK18 and labeled for G-actin (Alexa-Fluor-488–DNase1). (**K′–N′**) The same growth cones as in **K″–N″** labeled for F-actin with Alexa-Fluor-546–phalloidin. (**K″–N″**) Merged images of G-actin (green) and F-actin labeling (red). (**O**) Fluorescence intensity measurements of G-actin and F-actin labeling in growth cones treated with PAK18. (**P**) G-/F-actin ratiometric measurements of growth cones treated with PAK18. $^{**}P<0.01$, $^{***}P<0.001$, Kruskal–Wallis test with Dunn's *post-hoc* analysis, $n\geq35$. Scale bars: 10 µm.

area, we also measured total protein content in growth cones treated with PAK18 (supplementary material Fig. S4). Despite the morphological changes that accompany PAK18 stimulation, the growth cone total protein content remained constant at all doses (supplementary material Fig. S4A′–D′,F), while the ratio of p-XAC/total protein decreased in a dose-dependent manner (supplementary material Fig. S4A‴–D‴,G). It is noteworthy that 1 µM PAK18, which strongly stimulated axon outgrowth, only modestly reduced p-XAC, whereas higher levels of PAK18 strongly reduced p-XAC and inhibited outgrowth (Fig. 3A–E). This is consistent with the notion that balanced ADF/cofilin activity is necessary for optimal axon outgrowth, and slight variations across a growth cone can promote attractive or repulsive turning (Marsick et al., 2010). In contrast, p-MLC levels were strongly reduced at 1 µM PAK18, with modest further loss at higher levels of PAK18 (Fig. 3F–J). As with the p-XAC staining, we measured the total protein content in growth cones after PAK18 stimulation to ensure that the changes occurring after PAK18 stimulation were not due to changes in growth cone morphology (supplementary material Fig. S5).

Since active ADF/cofilin is known to depolymerize F-actin, we examined the relative levels of monomeric actin (G-actin) versus filamentous actin (F-actin) after treatment of 1, 10 and 50 µM PAK18. Neurons treated for 5 minutes with PAK18 were co-labeled for G-actin using Alexa-Fluor-488–DNase I and F-actin with Alexa-Fluor-546–phalloidin (Fig. 3K–P). Because DNase I binds actin monomers with high affinity relative to actin filaments (Hitchcock, 1980), whereas phalloidin only binds F-actin, we compared the relative abundance of both labels to assess the state of growth cone actin (Marsick et al., 2010). At 1 µM PAK18, we observed only a modest increase in the G/F actin ratio in growth cones (Fig. 3L,O,P), whereas at higher PAK18 concentrations there was a significant increase in G-actin labeling and an increase in the G/F-actin ratio (Fig. 3M–P). Together these results suggest that enhanced outgrowth at low concentrations of PAK18 is due to modest changes in G/F actin coupled with strong inhibition of myosin-II, whereas inhibition of outgrowth at high PAK18 is due to ADF/cofilin-mediated actin depolymerization.

If PAK18 inhibits myosin-II, we expected retrograde actin flow to be reduced. Retrograde actin flow is a process whereby actin filaments are drawn rearward because of the pulling force of myosin motors combined with the pushing force of polymerizing actin filaments against the plasma membrane (Dent et al., 2011; Lowery and Van Vactor, 2009). To examine whether PAK18 modulates retrograde F-actin flow, we labeled live neurons with tetramethylrhodamine-conjugated kabiramide-C (TMR–KabC) (Petchprayoon et al., 2005; Tanaka et al., 2003). TMR–abC is a small, cell-permeable molecule that binds to the barbed end of polymerizing actin filaments and has been used previously at low doses to track the rearward flow of actin filaments (Keren et al., 2008; Santiago-Medina et al., 2011). To label the plus ends of actin filaments, we treated neurons for 3 minutes with 3 nM TMR–KabC, which rapidly labels neurons, but does not affect the basal rate of neurite outgrowth or growth cone morphology (not shown). Immediately after TMR–KabC labeling, we imaged growth cones on LN at 2 second intervals by TIRF microscopy for 5 minutes before and after PAK18 stimulation (Fig. 4A,C; supplementary material Movie 3). In control conditions the rate of retrograde flow on LN was ~10.6 µm/minute (Fig. 4B,E), which is consistent with previous measurements (Chan and Odde,

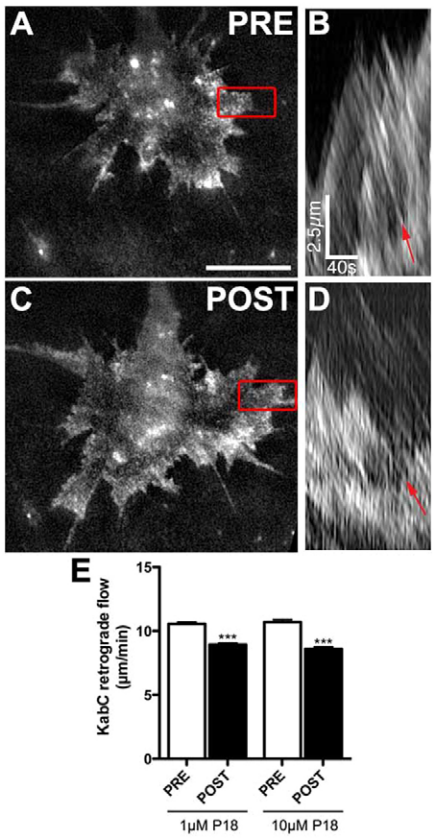

Fig. 4. Acute inhibition of PAK–PIX interactions decelerates F-actin retrograde flow. (**A**) A live growth cone labeled with the F-actin barbed-end binding probe, TMR–KabC. The red box denotes the region used to generate a kymograph (see Materials and Methods). (**B**) Kymograph from the boxed region of the growth cone in A indicating the rearward flow of KabC-capped actin filaments (red arrow). Note that the angle of flow lines indicates the rate of retrograde flow. (**C**) Growth cone in A, 5 minutes after stimulation with 1 µM PAK18. (**D**) Kymograph from the boxed region of the growth cone in C. Note the retrograde flow lines appear more shallow (red arrow), indicating the rate of actin rearward flow is reduced by 1 µM PAK18. (**E**) The average rate of retrograde flow is significantly reduced by both 1 and 10 µM PAK18. ***$P<0.001$, Kruskal–Wallis test with Dunn's *post-hoc* analysis, $n=10$. Scale bar: 10 µm (A,C).

2008; Marsick et al., 2010). However, upon treatment with PAK18, we observe an immediate reduction in the rate of retrograde flow (Fig. 4D,E), consistent with the inhibition of PAK-mediated myosin-II activity by PAK18. It is interesting to note that we observed similar rates of retrograde flow after treatment with 1 µM and 10 µM PAK18 (Fig. 4E), which is consistent with similar p-MLC labeling at these doses of PAK18 (Fig. 3G,H,J). These results further suggest that the inhibitory effects of PAK18 on axon outgrowth is due to the strong activation of ADF/cofilin at 10 µM (Fig. 3C,E).

PAK regulates growth cone point-contact formation and turnover

PAK regulates focal adhesion formation and turnover in crawling cells through phosphorylation of serine 273 of paxillin (S273-PXN), which requires binding of the PAK–PIX complex to paxillin through GIT (Brown et al., 2002; Deakin and Turner, 2008; Nayal et al., 2006; Turner et al., 1999). Since growth cone

motility is tightly linked to adhesion dynamics (Marsick et al., 2012; Myers and Gomez, 2011; Myers et al., 2011; Robles and Gomez, 2006; Santiago-Medina et al., 2011; Woo and Gomez, 2006; Woo et al., 2009) and modulating PAK function has dose-dependent effects on outgrowth (Fig. 2), we asked whether PAK18 also influences growth cone PCs. To test the effects of PAK18 on endogenous PCs, we stimulated growth cones with varying concentrations of PAK18 and immunolabeled for phosphorylated Y118-PXN (Fig. 5A–G). pY118-PXN is an excellent marker for mature adhesions (Deakin and Turner, 2008; Zaidel-Bar et al., 2007), which we have previously demonstrated to label *Xenopus* growth cone PCs (Robles and Gomez, 2006). Using particle analysis of thresholded ICC images, we found a dose-dependent increase in PC number, size and total intensity within growth cones treated with PAK18 (Fig. 5A–G). These results suggest that PAK18 promotes PC assembly and might reduce point contact turnover at high concentrations.

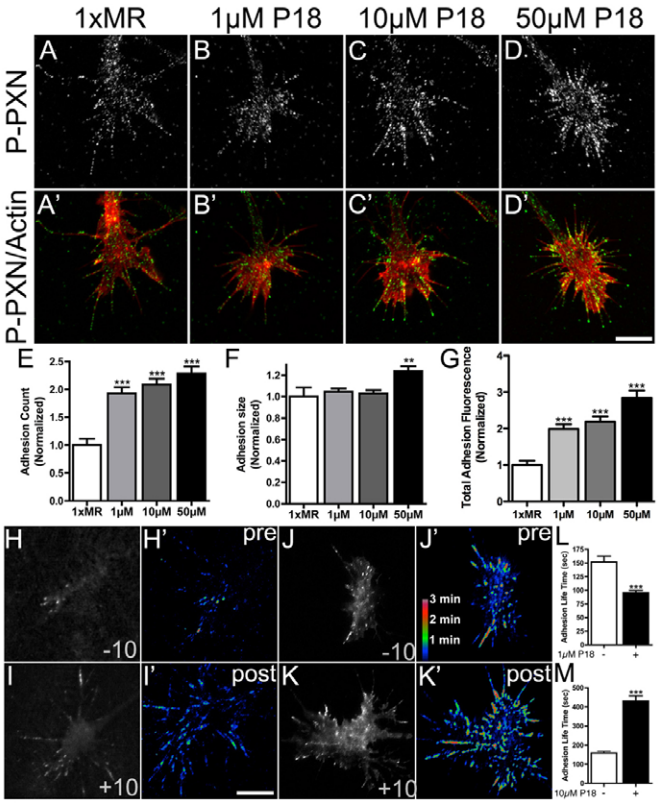

Fig. 5. Acute inhibition of PAK–PIX interactions regulates point contact formation and turnover. (**A–D**) Representative growth cones treated for 5 minutes with control medium or increasing concentrations of PAK18 and immunolabeled for p-PXN (Tyr118). (**A′–D′**) Merged images of p-PXN (green) and F-actin labeling (red). (**E–G**) Quantification of adhesions using particle analysis (see Materials and Methods) of p-PXN-labeled growth cones normalized to untreated control growth cones. $^{**}P<0.01$, $^{***}P<0.001$, Kruskal–Wallis test with Dunn's *post-hoc* analysis, $n\geq29$. (**H**,**I**) Time-lapse TIRF images of a live growth cone expressing PXN–GFP shown 10 minutes before (H) and after (I) stimulation with 1 μM PAK18. (**H′–I′**) Pseudocolored heat maps (see Materials and Methods), which illustrate point contact lifetimes over the 15 minute periods before and after stimulation with 1 μM PAK18. Note that many adhesions with short lifetimes form after 1 μM PAK18. (**J**,**K**) Time-lapse TIRF images of a live growth cone expressing PXN–GFP shown 10 minutes before (J) and after (K) stimulation with 10 μM PAK18. (**J′–K′**) Pseudocolored heat maps, which illustrates point contact lifetimes over the 15 minute periods before and after stimulation with 10 μM PAK18. Note that many adhesions with long lifetimes form after 10 μM PAK18. (**L–M**) Point contact adhesion lifetimes measured before and after stimulation with 1 μM PAK18 (L) and 10 μM PAK18 (M). $^{***}P<0.001$, Kruskal–Wallis test with Dunn's *post-hoc* analysis, $n=10$. Scale bar: 10 μm.

To directly test whether PAK18 regulates adhesion formation and turnover, we performed time-lapse TIRF imaging of paxillin–GFP (PXN–GFP) in living growth cones on LN during stimulation with PAK18 (Fig. 5H–M). Acute treatment with 1 μM PAK18 stimulated the rapid assembly of new PCs and accelerated PC turnover (Fig. 5H–I; supplementary material Movie 4). As the increase in the number of PCs/growth cone exceeds the expanded growth cone area, there is a greater than 50% increase in PC density (3.9 ± 0.3 adhesions/100 μm^2 pre-PAK18 versus 6.5 ± 0.3/100 μm^2 post-PAK18), which is also apparent in immunolabeled images (Fig. 5A–D). Moreover, at 1 μM PAK18, new PCs have a shorter adhesion lifetime (Fig. 5L). Other characteristics of point contacts, such as size and shape do not significantly change in presence of 1 μM PAK18. In contrast, while treatment with 10 μM PAK18 also stimulates the assembly of new PCs, these adhesions have a considerably longer lifetime and often cluster into larger aggregates, suggesting they are more mature adhesions (Fig. 5J,K,M; supplementary material Movie 5). Interestingly, the biphasic effects of PAK18 on adhesion lifetime correlates with the effects we observe on the rate of axon outgrowth and are consistent with previous findings that rapid turnover of PCs is associated with fast axon outgrowth (Myers and Gomez, 2011; Robles and Gomez, 2006; Woo and Gomez, 2006). The dose-dependent effects of PAK18 might be due to a partial displacement of PAK from PCs, as well as effects on actin polymerization and myosin activity.

To directly assess the effects of PAK18 on PAK localization to PCs, we imaged growth cones expressing both PXN–GFP and mCH–PAK3 during stimulation with 10 μM PAK18 (Fig. 6; supplementary material Movie 6). Prior to PAK18 treatment, PAK3 translocated to PXN-containing PCs with a short delay and typically dissociates from PCs before PXN is lost (Fig. 6A,C), suggesting that PAK has a transient function at adhesions. However, in the presence of 10 μM PAK18, the amount of PAK3 localizing to PXN-based adhesions was reduced significantly (Fig. 6E; $P<0.001$) and the time that PAK3 is associated with PXN was shortened dramatically relative to long PXN adhesion lifetime. Although less PAK3 localized to PCs in the presence of PAK18, low levels of PAK3 remained at PCs longer (Fig. 6F), suggesting that increased paxillin lifetime is sufficient to target PAK3 to adhesions.

Serine 273 paxillin phosphorylation regulates adhesion dynamics and growth cone motility

PAK regulates focal adhesion formation and turnover in part through phosphorylation of S273-PXN in crawling cells (Nayal et al., 2006). Because of the robust effects of PAK18 on PC dynamics (Figs 5, 6), we reasoned that phosphorylation of S273-PXN might modulate PC turnover to regulate growth cone motility. To examine the role of S273-PXN phosphorylation by PAK, we imaged adhesion dynamics and motility of growth cones overexpressing either phosphomimetic (S273D-PXN–GFP) or non-phosphorylatable (S273A-PXN–GFP) paxillin (Fig. 7). We first examined the effects of S273D-PXN on

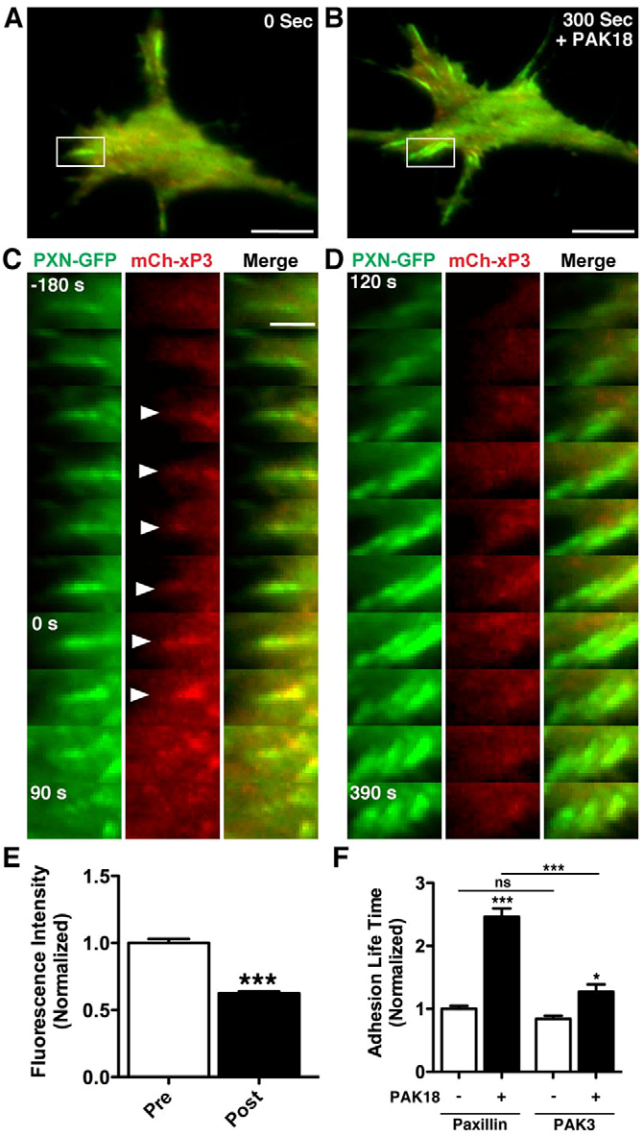

Fig. 6. Acute inhibition of PAK–PIX interactions displaces PAK from paxillin-based adhesions. (**A**,**B**) TIRF images of a live growth cone expressing both PXN–GFP and mCh–xPAK3 before (A) and after (B) stimulation with 10 µM PAK18. The white boxes indicate point contacts. (**C**,**D**) TIRF images of point contacts from boxed regions in A and B presented at 30 second intervals. Before PAK18 addition at 0 seconds, PXN targets to stable point contacts, which colocalize, with some delay, with PAK3 (arrowheads). However, upon addition of PAK18 at 0 seconds, PAK3 is lost from point contacts. In the continued presence of PAK18 (D), new point contacts recruit little PAK3 and are long lived. (**E**) Measurement of mCh–xPAK3 fluorescence at PXN–GFP point contacts shows reduced PAK3 after PAK18 addition. ***$P<0.001$, Student's *t*-test, $n>134$ point contacts in seven growth cones. (**F**) Measurement of point contact adhesion lifetimes shows that PXN and PAK3 remain within point contacts longer after PAK18. *$P<0.05$, ***$P<0.001$, Kruskal–Wallis test with Dunn's *post-hoc* analysis, $n=72$ point contacts in seven growth cones. Scale bars: 5 µm (A,B); 2 µm (C).

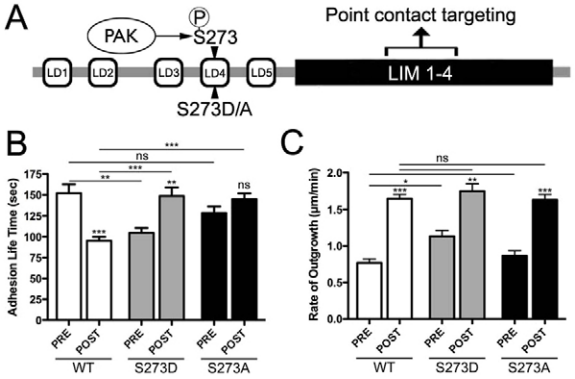

Fig. 7. S273 paxillin regulates point contact adhesion dynamics and growth cone motility. (**A**) Schematic diagram of paxillin showing the position of the S273 residue that is phosphorylated by PAK and was mutated to generate phosphomimetic (S273D) and nonphosphorylatable (S273A) variants of paxillin. (**B**) From time-lapse TIRF images of S273D/A-PXN–GFP, the lifetime of point contacts was measured before and after stimulation with 1 µM PAK18 in growth cones expressing wild-type and mutant variants of PXN. $n=10$. (**C**) The rate of neurite outgrowth 15 minutes before and after stimulation with 1 µM PAK18 in growth cones expressing wild-type and mutant variants of PXN. *$P<0.05$, **$P<0.01$, ***$P<0.001$, Kruskal–Wallis test with Dunn's *post-hoc* analysis, $n\geq38$.

baseline adhesion dynamics and growth cone motility. Consistent with the effects of phosphomimetic paxillin on focal adhesions and fibroblast migration (Nayal et al., 2006), growth cones expressing S273D-PXN–GFP had shorter PC lifetimes (Fig. 7B) and increased motility compared with wild-type neurons (Fig. 7C). This result suggests that increasing adhesion turnover with S273D-PXN is sufficient to modestly accelerate neurite outgrowth. We also tested the effects of the non-phosphorylatable, S273A-PXN, on growth cone PC turnover and neurite outgrowth. Unexpectedly, neither PC turnover, nor rate of neurite outgrowth were significantly different in S273A-PXN-expressing neurons (Fig. 7B,C). These results suggest that although paxillin phosphorylation at S273 may promote adhesion turnover and growth cone motility, phosphorylation at this site could be low under basal neurite outgrowth conditions on LN.

Next we examined how neurons expressing S273-paxillin mutants respond to partial PAK inhibition with 1 µM PAK18. Although 1 µM PAK18 normally shortens adhesion lifetime and accelerates neurite outgrowth of wild-type neurons, we found that 1 µM PAK18 significantly increased adhesion lifetime in S273D-PXN–GFP-expressing neurons and partially increased lifetime in S273A-PXN–GFP-expressing neurons (Fig. 7B; $P<0.001$). However, despite slowing adhesion turnover, PAK18 still stimulated neurite outgrowth in both S273D- and S273A-PXN–GFP-expressing neurons. This unexpected result suggests that inhibition of PAK with PAK18 probably promotes neurite extension by modulating multiple downstream cellular processes that are independent of S273-paxillin phosphorylation.

PIX-binding mutants of PAK suppress the effects of PAK18 and inhibit baseline growth cone motility

Our evidence suggests that PAK–PIX interactions have diverse affects on various cellular processes that control growth cone motility. However, PAK18 could have off-target effects, so determining the specificity of this peptide is crucial to conclusions regarding PAK function in growth cones. To address the specific function of PAK–PIX interactions in growth cones, we generated PAK constructs with mutated PIX binding motifs (Fig. 8A) that prevent PIX binding in other systems (Bagrodia et al., 1998; Bisson et al., 2007; Manser et al.,

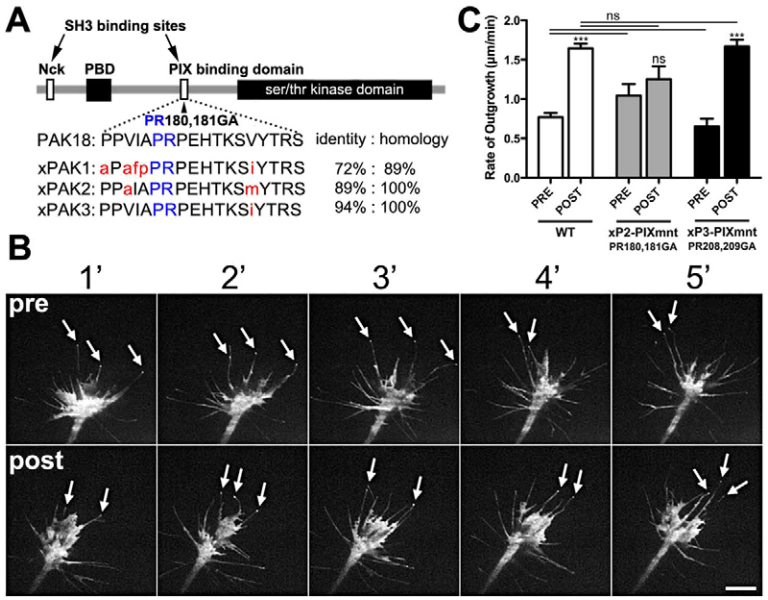

Fig. 8. A PIX-binding PAK2 mutant blocks the effects of PAK18. (**A**) Schematic diagram of PAK showing the PIX-binding domain and amino acid mutations that disrupt PAK binding to PIX. The PIX-binding domain of all three PAK isoforms is compared with the sequence of PAK18. Note strong sequence homology between PAK18 and xPAK2 and xPAK3, but less homology with xPAK1. Red indicate sequence divergence; blue indicates the amino acids necessary for PAK–PIX binding. (**B**) Time-lapse TIRF images of a growth cone expressing GFP–xPAK2-PR180,181GA (GFP–xP2-PIXm) shown at 1 minute intervals for 5 minutes before and after stimulation with 1 μM PAK18. Note that GFP–xP2-PIXm does not localize to point contacts, but does localize to filopodia tips (arrows), even after PAK18 treatment (lower panel). Also, note little morphological effect on GFP–xP2-PIXm-expressing growth cone after 1 μM PAK18. (**C**) Rate of neurite outgrowth measured 15 minutes before and after stimulation with 1 μM PAK18. ***$P<0.001$, Kruskal–Wallis test with Dunn's *post-hoc* analysis, $n \geq 22$. Scale bar: 10 μm.

1998). We generated point mutants of xPAK2 (xPAK2-PR180,181GA) and xPAK3 (xPAK3-PR208,209GA), because these isoforms are most homologous to PAK18 (Fig. 8A) and are more highly expressed in spinal neurons (Fig. 1). Consistent with a loss of PIX binding, we found by time-lapse TIRF imaging that GFP–xPAK2-PR180,181GA did not associate with adhesions, but still localized to the tips of extending filopodia (Fig. 8B). A similar PIX-binding mutant of xPAK3 did not target to stable PCs or filopodial tips, but appeared as a cytosolic volume marker in growth cones (not shown).

If PAK18 affects growth cones by disrupting PAK binding to PIX, then expressing, in neurons, PAK mutants deficient in PIX binding should block the effects of PAK18. Consistent with our previous results, suggesting that PAK–PIX interactions regulate growth cone motility, we found that expressing PIX-binding mutants of PAK alters axon outgrowth. Interestingly, the xPAK2 and xPAK3 PIX-binding mutants have distinct effects on the basal motility of growth cones, consistent with differing roles for PAK proteins in the regulation of cell motility (Bright et al., 2009). Neurons expressing GFP–xPAK2-PR180,181GA had faster rates of outgrowth than wild-type neurons, whereas the xPAK3 PIX-binding mutant had no effect on basal neurite outgrowth (Fig. 8C). In addition, expressing the xPAK2 PIX-binding mutant blocked the stimulatory effects of PAK18, whereas the xPAK3 PIX-binding mutant growth cones still accelerated in response to PAK18 (Fig. 8C). Taken together, these results suggest that xPAK2 most strongly influences growth cone motility through its interactions with PIX.

PAK and Rac1 compete for PIX binding

PAK and Rac1 are known to compete for a common binding site on PIX (ten Klooster et al., 2006), and PAK has been shown to act both downstream (Bokoch, 2003) and upstream of Rac1 activation (Obermeier et al., 1998), suggesting that the effects of PAK18 may be Rac1 dependent. To assess the role of Rac1 in response to PAK18, we expressed dominant-negative T17NRac1 (DN-Rac1) and stimulated mutant neurons with PAK18 during time-lapse imaging. DN-Rac1 inhibits endogenous Rac1 by sequestering the GEFs that normally activate Rac1 (Woo and Gomez, 2006). Consistent with an important role for Rac1, neurite outgrowth by DN-Rac1-expressing neurons was not significantly stimulated in response to PAK18, although a partial acceleration still occurred (supplementary material Fig. S6B). This result suggests that Rac1 activity is suppressed by PIX binding and that PAK18 releases active Rac1 to promote axon outgrowth. Moreover, this result is also consistent with the notion that some PAK remains active, which requires Rac1, at low levels of PAK18. To directly assess changes in Rac1 activity in response to PAK18, we used an antibody that specifically recognizes active, GTP-bound Rac1 (see Materials and Methods). Neurons were fixed after a 2-minute treatment with 1 μM PAK18, during the time when membrane protrusion is enhanced and axon outgrowth has accelerated (Fig. 2). ICC labeling for active GTP–Rac1 showed that Rac1 labeling increased in growth cones treated with PAK18 (supplementary material Fig. S6C–E). To assess the specificity of this antibody, we repeated this experiment in neurons expressing DN-Rac1. DN-Rac1-expressing neurons have reduced basal active Rac1 labeling relative to control neurons within the same dish (supplementary material Fig. S6F–H) and Rac1 labeling was not increased by PAK18 in DN-Rac1-expressing neurons. Together these data show that PAK18 rapidly activates Rac1 in neurons, which is necessary for the outgrowth-stimulating effects of this peptide.

Discussion

PAKs are multi-target serine/threonine kinases that regulate cell motility through several distinct molecular mechanisms. Here we provide the first detailed study of PAK function in developing neuronal growth cones. We show that PAK1 is weakly expressed, but PAK2 and PAK3 are highly expressed in developing spinal neurons and localize to distinct regions within motile growth cones. Both PAK2 and PAK3 colocalize with the adaptor protein PIX at paxillin-containing point contacts, whereas only PAK2 targets to filopodial tips independent of PIX. The acute disruption of the PAK–PIX interactions with the cell-permeable peptide, PAK18, has robust, dose-dependent effects on growth cone morphology and motility. A low dose of PAK18 strongly stimulated neurite outgrowth by partially activating ADF/cofilin

and inhibiting myosin-II, which promotes membrane protrusion and dynamic point contact assembly. In contrast, a high dose of PAK18 strongly inhibited growth cone motility, probably through full activation of ADF/cofilin leading to actin filament depolymerization. Expressing specific PAK mutants in neurons confirmed the specificity of the PAK18 peptide and demonstrates a role for PAK phosphorylation of S273-paxillin in the regulation of adhesion dynamics. Lastly, our evidence suggests that Rac1 activity is controlled in part through PAK and PIX interactions in growth cones.

PAK distribution in growth cones

The distribution of PAK proteins is dynamic and varied within growth cones. The distinct localizations of PAK isoforms may target PAK activity to specific downstream effectors. For example, xPAK2 localized to both paxillin adhesions and to the tips of extending filopodia (Fig. 1) suggesting a role in adhesion function and actin polymerization at filopodial tips. Functional evidence suggests that xPAK2 promotes filopodial extension, as low-dose PAK18 stimulated filopodial production (Fig. 2H), possibly by displacing active PAK away from point contacts to filopodial tips. This is consistent with previous studies implicating PAK signaling in the regulation of both axonal and dendritic filopodial extension (Heckman et al., 2009; Kayser et al., 2008; Robles et al., 2005). These results suggest that PAK2 regulates actin filament polymerization, but the relevant targets of PAK at filopodial tips remain unknown. xPAK3 was restricted to point contacts, suggesting an overlapping function with xPAK2 in the regulation of adhesion dynamics (see below), but not with actin polymerization at filopodial tips. Interestingly, xPAK1 does not concentrate at either point contacts or filopodial tips, suggesting this family member is missing key targeting sequences contained in PAK2/3.

PAK regulation of the growth cone cytoskeleton

Two of the best known downstream targets of PAK function are ADF/cofilin and myosin-II (supplementary material Fig. S7A). Active PAK inhibits ADF/cofilin through LIM kinase, which phosphorylates cofilin at serine 3 (Sarmiere and Bamburg, 2004). Interestingly, we observed a robust stimulation of axon outgrowth after partial activation (dephosphorylation) of ADF/cofilin with 1 μM PAK18, but complete inhibition of outgrowth after strong ADF/cofilin activation with 50 μM PAK18 (Fig. 3A–E; supplementary material Fig. S7C,F). Consistent with actin depolymerization by ADF/cofilin, we observed a corresponding loss of F-actin with increasing PAK18 concentration (Fig. 3K–P). Stimulation of axon outgrowth at low PAK18 could be due to partial severing of actin filaments to generate new free barbed ends, together with increased globular actin that promotes polymerization at the leading edge (Ichetovkin et al., 2002). PAK18 also reduced myosin-II activity (Fig. 3F–J), which could stimulate growth cone motility by slowing retrograde actin flow (Fig. 4; supplementary material Fig. S7C,F). However, the inhibitory effects of high PAK18 are probably not due to stronger myosin inhibition, as we observed only a modest further decrease in both myosin-II dephosphorylation (Fig. 3J) and retrograde flow of actin (Fig. 4) at higher PAK18. Recent evidence also suggests that active ADF/cofilin directly inhibits myosin-II binding to F-actin (Wiggan et al., 2012), which could further account for the decrease in myosin-II activity downstream of high PAK18. It remains to be determined whether the subcellular targeting of different PAK isoforms in growth cones controls the activation of specific effector pathways. Interestingly, our results are consistent with the effects of inhibiting RhoA kinase (ROCK) on neurite outgrowth. ROCK regulates ADF/cofilin and myosin-II similar to PAK and stimulates filopodial and lamellipodial extension in growth cones when inhibited (Loudon et al., 2006). ROCK inhibition has also been reported to potentiate both the size and motility of growth cones (Bito et al., 2000), suggesting that partial inhibition of PAK may effect common targets to ROCK in neuronal growth cones.

PAK regulation of growth cone point contacts

One critical determinant of the speed and direction of cell motility is the assembly and dynamic turnover of substratum adhesion sites (Myers and Gomez, 2011; Myers et al., 2012; Myers et al., 2011; Wu et al., 2012). Although the role of PAK in adhesion-dependent motility of non-neuronal cells has been extensively studied (Bokoch, 2003; Rosenberger and Kutsche, 2006), almost nothing is known about PAK function in adhesion dynamics in growth cone motility and axon pathfinding. Interestingly, the acute disruption of PAK–PIX interactions with PAK18 lead to dose-dependent, biphasic changes in growth cone point contact turnover that closely mirror motility (supplementary material Fig. S7E). Low PAK18 stimulates the assembly of many new point contacts that have shorter lifetimes (Fig. 6H,I,L) and neurite outgrowth accelerates. Alternatively, high PAK18 causes point contacts to become over-stabilized and neurite outgrowth stalls (supplementary material Fig. S7E). There are several possible explanations for the effects we see on adhesion turnover. At low PAK18, a partial inhibition of myosin may promote growth cone motility by accelerating adhesion turnover, as myosin activity is necessary for focal adhesion maturation (Kuo et al., 2011; Woo and Gomez, 2006). In addition, PAK association with PIX has been shown to stabilize adhesions in breast cancer cells (Stofega et al., 2004), and PAK phosphorylation of PXN promotes adhesion turnover (Nayal et al., 2006), so partial dissociation of PAK from adhesions may destabilize point contacts, but not prevent adhesion reassembly. Moreover, our data suggests that Rac1 is activated by PAK18 (supplementary material Fig. S6), which is known to promote new adhesion formation within nascent protrusions (ten Klooster et al., 2006; Woo and Gomez, 2006). However, the inhibitory effects of 10 μM PAK18 on adhesion turnover in wild-type cells is more difficult to explain, but is probably the result of strong inhibition of PAK function (supplementary material Fig. S7E). Some PAK activity may be necessary for adhesion turnover through PXN phosphorylation at S273, so strong loss of PAK from adhesions at 10 μM PAK18 may stabilize adhesions because of a lack of PAK-dependent phosphorylation of PXN (supplementary material Fig. S7E). Consistent with this notion, we found that there was increased adhesion turnover of growth cones expressing phosphomimetic S273D-PXN (Fig. 7B) and faster neurite outgrowth (Fig. 7C), suggesting that rapid adhesion turnover is sufficient to potentiate outgrowth. However, although S273D-PXN-expressing neurons do not exhibit increased adhesion turnover in response to PAK18, they do accelerate their rate of neurite outgrowth, suggesting that several independent pathways promote neurite outgrowth downstream of PAK18. The effects of non-phosphorylatable S273A-PXN on PC lifetime and neurite outgrowth in response to PAK18

dissociate changes in adhesion turnover from neurite acceleration. These results indicate that PAK18-mediated neurite outgrowth must be working independently of paxillin phosphorylation at S273 and that perhaps adhesion turnover is primarily mediated by the cytoskeletal changes triggered by PAK18. It should also be noted that we do observe modest effects of PAK18 on leading edge protrusion of growth cones on PDL (Fig. 2E), suggesting some PAK–PIX interactions occur without integrin engagement. Given the complex interplay between a number of signaling pathways, clearly the role of PAK in the control of growth cone adhesion dynamics requires further study.

PAK in axon guidance

PAK is implicated in axon guidance downstream of both attractive and repulsive cues (Aizawa et al., 2001; Fan et al., 2003; Lucanic et al., 2006; Shekarabi et al., 2005). For example, Netrin-1 stimulates growth-cone expansion through PAK1 (Shekarabi et al., 2005) and inhibition of PAK kinase activity permits axon extension over repulsive ECM molecules (Marler et al., 2005). The distinct cellular distributions of multiple PAK family members in growth cones and numerous functional targets of PAK proteins may explain how PAK functions downstream of positive and negative guidance cues. Moreover, correct axon targeting requires both PAK kinase activity and association with the adaptor protein Nck (Ang et al., 2003; Hing et al., 1999). The regulation of filopodial extension by PAK may also influence growth cone guidance (Kim et al., 2003; Robles et al., 2005). Because guidance cue receptors cluster at the tips of filopodia (Galbraith et al., 2007; Shafer et al., 2011), they serve as important sensory extensions of growth cones (Chien et al., 1993). By regulating filopodial protrusion, PAK may regulate the exploratory behavior of growth cones. Stimulation of filopodial extensions at low PAK18 may be due to a redistribution of active PAK to filopodial tips (Fig. 2F,H), which is consistent with our previous findings showing that PAK regulates filopodial tip elongation (Robles et al., 2005). In a related cellular specialization, PAK1 and 3 appear pivotal in the development of dendritic spines, as over-activation of PAK1/3 increases spines (and filopodia), whereas PAK loss of function, or expression of mutant PAK proteins prevents spine formation and maturation (Boda et al., 2004; Zhang et al., 2005). It is noteworthy that the signaling complex consisting of GIT1, PIX, Rac and PAK, which our evidence suggests operates to control growth cone motility, also functions in spine morphogenesis (Zhang et al., 2005). Importantly, point mutations in brain-specific PAK family members in humans lead to abnormal spines *in vivo*, which is associated with non-syndromic X-linked mental retardation (MRX) (Boda et al., 2004; Raymond, 2006).

Concluding remarks

This study is focused on understanding the integrative function of PAK on the actin cytoskeleton and paxillin-based adhesions of motile growth cones. It demonstrates a role for PAK in cytoskeletal remodeling and adhesion dynamics, two critical regulators of axon outgrowth and pathfinding in the developing nervous system. Mutations in genes involved in detecting and transducing axon guidance information into directed neurite outgrowth are probably responsible for many deficits in cognitive function, including autisms, dyslexias and mental retardations. By studying how fundamental proteins, such as PAK, regulate cell motility and affect the dynamic process of brain development, we hope to better understand both the normal function of these proteins and identify potential sites for therapeutic intervention. Given the strong axon-outgrowth-promoting effects of PAK18, modulating PAK function using cell-permeable peptides may be a useful strategy to enhance axon regeneration after injury.

Materials and Methods

RT-PCR and primers

PAK primers were designed by inserting the corresponding *Xenopus laevis* genomic sequences, obtained from Xenbase (Bowes et al., 2010) into Primer3 (Rozen and Skaletsky, 2000). The designed PAK primers were synthesized at the Biotechnology Center of the University of Wisconsin–Madison. PAK transcripts were amplified from reverse transcribed RNA isolated from stage 25–26 (Nieuwkoop and Faber, 1994) embryo spinal cords. The total RNA was first isolated from 15–20 spinal cords with TRIzol (Invitrogen) and made into cDNA through RT-PCR using random decamers as primers.

Plasmid constructs

All expression constructs were subcloned into the *Xenopus*-preferred pCS2+ vector for mRNA synthesis (Dave Turner, University of Michigan, Ann Arbor, MI). Gateway technology (Invitrogen, Carlsbad, CA) was used in some cases to generate pCS2+ constructs. cDNAs for chicken paxillin–GFP and paxillin-S273D/A were provided by A. F. Horwitz (University of Virginia, Charlottesville, VA). *Xenopus* isoforms of wild-type PAK1, PAK2 and PAK3 constructs were provided by Tom Moss (University of Toronto, Ontario, Canada), Nathalie Morin (Centre de Recherche de Biochimie Macromoleculaire, France) and Jacob Souopgui (Université Libre de Bruxelles, Belgium). All cDNA clones were put into pCS2+ vectors using Gateway technology. The mutant constructs of xPAK2 (PR180,181GA) and xPAK3 (PR208,209GA) in the PIX-binding domain were generated using QuikChange Site Directed Mutagenesis (Agilent, Santa Clara, CA). Dominant negative Rac1 (DN-Rac1; T17N) was provided by Maureen L. Ruchhoeft and William A. Harris (University of Cambridge, UK).

Embryo injection and cell culture

Xenopus laevis embryos were obtained as described previously (Gómez et al., 2003) and staged according to Nieuwkoop and Faber (Nieuwkoop and Faber, 1994). For direct expression experiments using constructs, two dorsal blastomeres of eight-cell-stage embryos were injected with 0.25–0.5 ng of *in vitro*-transcribed, capped mRNA (mMessage Machine, Ambion, Austin, TX) or 60–80 pg DNA for paxillin–GFP. Neural tubes were dissected from 1-day-old embryos and explant cultures containing a heterogeneous population of spinal neurons were prepared as previously described (Gómez et al., 2003). Explants were plated onto acid-washed coverslips coated with 25 µg/ml laminin (LN; Sigma, St. Louis, MO) or 50 µg/ml poly-D-lysine (PDL; Sigma, St. Louis, MO). Cultures were imaged or fixed 16–24 h after plating. All methods were approved by the University of Wisconsin School of Medicine Animal Care and Use Committee.

Reagents

PAK18 (EMD Biosciences, Calbiochem, La Jolla, CA) was diluted in 1× MR (modified ringer) and perfused through cultures as described previously (Gómez et al., 2003). The control PAK18 peptide was synthesized by the University of Wisconsin Peptide Synthesis Facility (Madison, WI). The peptide was synthesized in the reverse order of PAK18, coupled to a TAT internalization sequence and purified by high-pressure liquid chromatography, and confirmed using mass spectrometry. Antibodies used were as follows: anti-xPAK1 and anti-xPAK2 (kind gift from Nathalie Morin, Universités Montpellier, France), anti-βPAK3 (N-19, Santa Cruz Biotechnology), anti-pS3-ADF/cofilin (pS3-XAC1; kind gift from James Bamburg, Colorado State University), anti-pS19-MLC2 (Cell Signaling Technology, Danvers, MA), anti-pY118-paxillin (Invitrogen), anti-βI,II-tubulin (Sigma), anti-Rac1–GTP (NewEast Biosciences, King of Prussia, PA). For monomeric G-actin staining, deoxyribonuclease I (Alexa-Fluor-488–DNase I; Invitrogen) was used. To visualize actin retrograde flow, neuronal cultures were incubated in 3 nM kabarimide C conjugated to tetramethylrhodamine (TMR–KabC; kind gift from Gerard Marriott, University of California, Berkeley) for 3 minutes, then washed with 1× MR.

Immunoblotting and immunocytochemistry

Immunoblotting for PAK proteins was performed as described previously (Robles et al., 2005). Total proteins were extracted from stage 25–26 embryo spinal cords. Five spinal cords were processed for each lane and run on a Novex NuPAGE SDS-PAGE gel (Invitrogen). Primary PAK1–3 antibodies were used at 1:1000. Horseradish peroxidase (HRP)-conjugated secondary antibodies (Jackson Immuno) were used at 1:5000 and the blots were visualized by enhanced chemiluminescence (Thermo Scientific Pierce ECL).

For immunocytochemistry (ICC), spinal neuron cultures were fixed in 4% paraformaldehyde in Krebs+sucrose fixative (4% PKS) (Dent and Meiri, 1992), permeabilized with 0.1% Triton X-100, and blocked in 1.0% fish gelatin in calcium- and magnesium-free PBS for 1 hour at room temperature. Primary antibodies were used at the following dilutions in blocking solution: 1:300 anti-pS3-XAC (Bamburg), 1:250 anti-pS19-MLC2 (Cell Signaling Technology), 1:500 anti-pY118-paxillin (Invitrogen), 1:500 anti-Rac1–GTP (NewEast Biosciences), 1:500 anti-βI,II-Tubulin (Sigma). Alexa-Fluor-conjugated secondary antibodies were purchased from Invitrogen and used at 1:250 in blocking solution. Included with secondary antibodies was Alexa-Fluor-546–phalloidin (1:100; Invitrogen) to label filamentous actin (F-actin) and Alexa-Fluor-647–carboxylic acid, succinimidyl ester (1:1000; Invitrogen) to label total protein.

Image acquisition and analysis

For both live and fixed fluorescence microscopy, high-magnification images were acquired using either a 60×/1.45 NA objective lens on an Olympus Fluoview 500 laser-scanning confocal system mounted on an AX-70 upright microscope or a 100×/1.5 NA objective lens on a Nikon total internal reflection fluorescence (TIRF) microscope. For confocal microscopy, samples were imaged at 2–2.5×zoom (pixel size=165–200 nm). Images were captured at 10–20 second intervals. For brightfield time-lapse microscopy, low-magnification phase-contrast images were acquired using a 20× objective on a Nikon microscope equipped with an x–y motorized stage for multi-positional imaging. Multi-positional images were capture at 1 minute intervals. Live explant cultures were sealed within perfusion chambers as described previously (Gómez et al., 2003) to allow rapid exchange of solutions. Images were analyzed using ImageJ software (W. Rasband, National Institutes of Health, Bethesda, MD). Point contacts were identified as discrete areas containing paxillin–GFP that were at least two times brighter than the surrounding background and remained fixed in place for a minimum of 30 seconds (Woo and Gomez, 2006). Measurements of p-Cofilin and p-MLCII or Rac1–GTP intensity were made by first selecting the perimeter of growth cones from thresholded F-actin-labeled or total-protein-labeled images based on intensity to exclude background, using ImageJ. These user-defined regions were then used to measure the average pixel intensity of immunolabeling within non-thresholded growth cones. For display purposes, some images were pseudo-colored using ImageJ look up tables.

Dynamic adhesion maps

Dynamic adhesion map images were prepared from image stacks as detailed previously (Santiago-Medina et al., 2011). Briefly, an image stabilization algorithm was applied if necessary and to improve edge detection an unsharp mask routine was applied, followed by thresholding to highlight the puncta of interest. Next, an 8-bit binary filter was applied to equalize point contact intensities. Image stacks were then converted to 16-bit and user-defined subsets were summed so that intensity was used as a measure of pixel lifetime. Final images were contrast enhanced and pseudo-colored.

Acknowledgements

We thank Kate Kalil, Erik Dent and members of the Gomez lab for comments on the manuscript.

Author contributions

M.S.-M. and T.M.G. designed the research; M.S.-M. and K.A.G. performed the research and analyzed the data; M.S.-M. and T.M.G. wrote the paper.

Funding

This work was supported by the National Institutes of Health [grant number NS41564 to T.M.G. and diversity supplement to M.S.M.]. Deposited in PMC for release after 12 months.

Supplementary material available online at
http://jcs.biologists.org/lookup/suppl/doi:10.1242/jcs.112607/-/DC1

References

Aizawa, H., Wakatsuki, S., Ishii, A., Moriyama, K., Sasaki, Y., Ohashi, K., Sekine-Aizawa, Y., Sehara-Fujisawa, A., Mizuno, K., Goshima, Y. et al. (2001). Phosphorylation of cofilin by LIM-kinase is necessary for semaphorin 3A-induced growth cone collapse. *Nat. Neurosci.* **4**, 367-373.

Ang, L. H., Kim, J., Stepensky, V. and Hing, H. (2003). Dock and Pak regulate olfactory axon pathfinding in Drosophila. *Development* **130**, 1307-1316.

Arias-Romero, L. E. and Chernoff, J. (2008). A tale of two Paks. *Biol. Cell* **100**, 97-108.

Bagrodia, S., Taylor, S. J., Jordon, K. A., Van Aelst, L. and Cerione, R. A. (1998). A novel regulator of p21-activated kinases. *J. Biol. Chem.* **273**, 23633-23636.

Bisson, N., Islam, N., Poitras, L., Jean, S., Bresnick, A. and Moss, T. (2003). The catalytic domain of xPAK1 is sufficient to induce myosin II dependent in vivo cell fragmentation independently of other apoptotic events. *Dev. Biol.* **263**, 264-281.

Bisson, N., Poitras, L., Mikryukov, A., Tremblay, M. and Moss, T. (2007). EphA4 signaling regulates blastomere adhesion in the Xenopus embryo by recruiting Pak1 to suppress Cdc42 function. *Mol. Biol. Cell* **18**, 1030-1043.

Bito, H., Furuyashiki, T., Ishihara, H., Shibasaki, Y., Ohashi, K., Mizuno, K., Maekawa, M., Ishizaki, T. and Narumiya, S. (2000). A critical role for a Rho-associated kinase, p160ROCK, in determining axon outgrowth in mammalian CNS neurons. *Neuron* **26**, 431-441.

Boda, B., Alberi, S., Nikonenko, I., Node-Langlois, R., Jourdain, P., Moosmayer, M., Parisi-Jourdain, L. and Muller, D. (2004). The mental retardation protein PAK3 contributes to synapse formation and plasticity in hippocampus. *J. Neurosci.* **24**, 10816-10825.

Bokoch, G. M. (2003). Biology of the p21-activated kinases. *Annu. Rev. Biochem.* **72**, 743-781.

Bowes, J. B., Snyder, K. A., Segerdell, E., Jarabek, C. J., Azam, K., Zorn, A. M. and Vize, P. D. (2010). Xenbase: gene expression and improved integration. *Nucleic Acids Res.* **38 Database issue**, D607-D612.

Bright, M. D., Garner, A. P. and Ridley, A. J. (2009). PAK1 and PAK2 have different roles in HGF-induced morphological responses. *Cell. Signal.* **21**, 1738-1747.

Brown, M. C., West, K. A. and Turner, C. E. (2002). Paxillin-dependent paxillin kinase linker and p21-activated kinase localization to focal adhesions involves a multistep activation pathway. *Mol. Biol. Cell* **13**, 1550-1565.

Carlstrom, L. P., Hines, J. H., Henle, S. J. and Henley, J. R. (2011). Bidirectional remodeling of β1-integrin adhesions during chemotropic regulation of nerve growth. *BMC Biol.* **9**, 82.

Cau, J., Faure, S., Vigneron, S., Labbé, J. C., Delsert, C. and Morin, N. (2000). Regulation of Xenopus p21-activated kinase (X-PAK2) by Cdc42 and maturation-promoting factor controls Xenopus oocyte maturation. *J. Biol. Chem.* **275**, 2367-2375.

Chan, C. E. and Odde, D. J. (2008). Traction dynamics of filopodia on compliant substrates. *Science* **322**, 1687-1691.

Chien, C. B., Rosenthal, D. E., Harris, W. A. and Holt, C. E. (1993). Navigational errors made by growth cones without filopodia in the embryonic Xenopus brain. *Neuron* **11**, 237-251.

Cobos, I., Borello, U. and Rubenstein, J. L. (2007). Dlx transcription factors promote migration through repression of axon and dendrite growth. *Neuron* **54**, 873-888.

Daniels, R. H., Hall, P. S. and Bokoch, G. M. (1998). Membrane targeting of p21-activated kinase 1 (PAK1) induces neurite outgrowth from PC12 cells. *EMBO J.* **17**, 754-764.

Deakin, N. O. and Turner, C. E. (2008). Paxillin comes of age. *J. Cell Sci.* **121**, 2435-2444.

Dent, E. W. and Meiri, K. F. (1992). GAP-43 phosphorylation is dynamically regulated in individual growth cones. *J. Neurobiol.* **23**, 1037-1053.

Dent, E. W., Gupton, S. L. and Gertler, F. B. (2011). The growth cone cytoskeleton in axon outgrowth and guidance. *Cold Spring Harb. Perspect. Biol.* **3**, a001800.

Fan, X., Labrador, J. P., Hing, H. and Bashaw, G. J. (2003). Slit stimulation recruits Dock and Pak to the roundabout receptor and increases Rac activity to regulate axon repulsion at the CNS midline. *Neuron* **40**, 113-127.

Galbraith, C. G., Yamada, K. M. and Galbraith, J. A. (2007). Polymerizing actin fibers position integrins primed to probe for adhesion sites. *Science* **315**, 992-995.

Godement, P., Wang, L. C. and Mason, C. A. (1994). Retinal axon divergence in the optic chiasm: dynamics of growth cone behavior at the midline. *J. Neurosci.* **14**, 7024-7039.

Gómez, T. M., Harrigan, D., Henley, J. and Robles, E. (2003). Working with Xenopus spinal neurons in live cell culture. *Methods Cell Biol.* **71**, 129-156.

Hayashi, K., Ohshima, T. and Mikoshiba, K. (2002). Pak1 is involved in dendrite initiation as a downstream effector of Rac1 in cortical neurons. *Mol. Cell. Neurosci.* **20**, 579-594.

Heckman, C. A., Demuth, J. G., Deters, D., Malwade, S. R., Cayer, M. L., Monfries, C. and Mamais, A. (2009). Relationship of p21-activated kinase (PAK) and filopodia to persistence and oncogenic transformation. *J. Cell. Physiol.* **220**, 576-585.

Hines, J. H., Abu-Rub, M. and Henley, J. R. (2010). Asymmetric endocytosis and remodeling of beta1-integrin adhesions during growth cone chemorepulsion by MAG. *Nat. Neurosci.* **13**, 829-837.

Hing, H., Xiao, J., Harden, N., Lim, L. and Zipursky, S. L. (1999). Pak functions downstream of Dock to regulate photoreceptor axon guidance in Drosophila. *Cell* **97**, 853-863.

Hitchcock, S. E. (1980). Actin deoxyroboncuclease I interaction. Depolymerization and nucleotide exchange. *J. Biol. Chem.* **255**, 5668-5673.

Ichetovkin, I., Grant, W. and Condeelis, J. (2002). Cofilin produces newly polymerized actin filaments that are preferred for dendritic nucleation by the Arp2/3 complex. *Curr. Biol.* **12**, 79-84.

Kayser, M. S., Nolt, M. J. and Dalva, M. B. (2008). EphB receptors couple dendritic filopodia motility to synapse formation. *Neuron* **59**, 56-69.

Keren, K., Pincus, Z., Allen, G. M., Barnhart, E. L., Marriott, G., Mogilner, A. and Theriot, J. A. (2008). Mechanism of shape determination in motile cells. *Nature* **453**, 475-480.

Kim, M. D., Kamiyama, D., Kolodziej, P., Hing, H. and Chiba, A. (2003). Isolation of Rho GTPase effector pathways during axon development. *Dev. Biol.* **262**, 282-293.

Kolodkin, A. L. and Tessier-Lavigne, M. (2011). Mechanisms and molecules of neuronal wiring: a primer. *Cold Spring Harb. Perspect. Biol.* **3**, a001727.
Kreis, P. and Barnier, J. V. (2009). PAK signalling in neuronal physiology. *Cell. Signal.* **21**, 384-393.
Kuo, J. C., Han, X., Hsiao, C. T., Yates, J. R., 3rd and Waterman, C. M. (2011). Analysis of the myosin-II-responsive focal adhesion proteome reveals a role for β-Pix in negative regulation of focal adhesion maturation. *Nat. Cell Biol.* **13**, 383-393.
Loudon, R. P., Silver, L. D., Yee, H. F., Jr and Gallo, G. (2006). RhoA-kinase and myosin II are required for the maintenance of growth cone polarity and guidance by nerve growth factor. *J. Neurobiol.* **66**, 847-867.
Lowery, L. A. and Van Vactor, D. (2009). The trip of the tip: understanding the growth cone machinery. *Nat. Rev. Mol. Cell Biol.* **10**, 332-343.
Lucanic, M., Kiley, M., Ashcroft, N., L'etoile, N. and Cheng, H. J. (2006). The Caenorhabditis elegans P21-activated kinases are differentially required for UNC-6/netrin-mediated commissural motor axon guidance. *Development* **133**, 4549-4559.
Manser, E., Loo, T. H., Koh, C. G., Zhao, Z. S., Chen, X. Q., Tan, L., Tan, I., Leung, T. and Lim, L. (1998). PAK kinases are directly coupled to the PIX family of nucleotide exchange factors. *Mol. Cell* **1**, 183-192.
Marín, O., Valiente, M., Ge, X. and Tsai, L. H. (2010). Guiding neuronal cell migrations. *Cold Spring Harb. Perspect. Biol.* **2**, a001834.
Marler, K. J., Kozma, R., Ahmed, S., Dong, J. M., Hall, C. and Lim, L. (2005). Outgrowth of neurites from NIE-115 neuroblastoma cells is prevented on repulsive substrates through the action of PAK. *Mol. Cell. Biol.* **25**, 5226-5241.
Marsick, B. M., Flynn, K. C., Santiago-Medina, M., Bamburg, J. R. and Letourneau, P. C. (2010). Activation of ADF/cofilin mediates attractive growth cone turning toward nerve growth factor and netrin-1. *Dev. Neurobiol.* **70**, 565-588.
Marsick, B. M., San Miguel-Ruiz, J. E. and Letourneau, P. C. (2012). Activation of ezrin/radixin/moesin mediates attractive growth cone guidance through regulation of growth cone actin and adhesion receptors. *J. Neurosci.* **32**, 282-296.
Maruta, H., He, H. and Nheu, T. (2002). Interfering with Ras signaling using membrane-permeable peptides or drugs. *Methods Mol. Biol.* **189**, 75-85.
Myers, J. P. and Gomez, T. M. (2011). Focal adhesion kinase promotes integrin adhesion dynamics necessary for chemotropic turning of nerve growth cones. *J. Neurosci.* **31**, 13585-13595.
Myers, J. P., Santiago-Medina, M. and Gomez, T. M. (2011). Regulation of axonal outgrowth and pathfinding by integrin-ECM interactions. *Dev. Neurobiol.* **71**, 901-923.
Myers, J. P., Robles, E., Ducharme-Smith, A. and Gomez, T. M. (2012). Focal adhesion kinase modulates Cdc42 activity downstream of positive and negative axon guidance cues. *J. Cell Sci.* **125**, 2918-2929.
Nayal, A., Webb, D. J., Brown, C. M., Schaefer, E. M., Vicente-Manzanares, M. and Horwitz, A. R. (2006). Paxillin phosphorylation at Ser273 localizes a GIT1-PIX-PAK complex and regulates adhesion and protrusion dynamics. *J. Cell Biol.* **173**, 587-589.
Nieuwkoop, P. D. and Faber, J. (1994). *Normal table of Xenopus laevis (Daudin)*. Garland, New York.
Obermeier, A., Ahmed, S., Manser, E., Yen, S. C., Hall, C. and Lim, L. (1998). PAK promotes morphological changes by acting upstream of Rac. *EMBO J.* **17**, 4328-4339.
Petchprayoon, C., Suwanborirux, K., Tanaka, J., Yan, Y., Sakata, T. and Marriott, G. (2005). Fluorescent kabiramides: new probes to quantify actin in vitro and in vivo. *Bioconjug. Chem.* **16**, 1382-1389.
Raymond, F. L. (2006). X linked mental retardation: a clinical guide. *J. Med. Genet.* **43**, 193-200.
Robles, E. and Gomez, T. M. (2006). Focal adhesion kinase signaling at sites of integrin-mediated adhesion controls axon pathfinding. *Nat. Neurosci.* **9**, 1274-1283.
Robles, E., Woo, S. and Gomez, T. M. (2005). Src-dependent tyrosine phosphorylation at the tips of growth cone filopodia promotes extension. *J. Neurosci.* **25**, 7669-7681.
Rosenberger, G. and Kutsche, K. (2006). AlphaPIX and betaPIX and their role in focal adhesion formation. *Eur. J. Cell Biol.* **85**, 265-274.
Rozen, S. and Skaletsky, H. (2000). Primer3 on the WWW for general users and for biologist programmers. *Methods Mol. Biol.* **132**, 365-386.
Santiago-Medina, M., Myers, J. P. and Gomez, T. M. (2011). Imaging adhesion and signaling dynamics in Xenopus laevis growth cones. **72**, 585-599. *Dev. Neurobiol*.
Sarmiere, P. D. and Bamburg, J. R. (2004). Regulation of the neuronal actin cytoskeleton by ADF/cofilin. *J. Neurobiol.* **58**, 103-117.
Shafer, B., Onishi, K., Lo, C., Colakoglu, G. and Zou, Y. (2011). Vangl2 promotes Wnt/planar cell polarity-like signaling by antagonizing Dvl1-mediated feedback inhibition in growth cone guidance. *Dev. Cell* **20**, 177-191.
Shekarabi, M., Moore, S. W., Tritsch, N. X., Morris, S. J., Bouchard, J. F. and Kennedy, T. E. (2005). Deleted in colorectal cancer binding netrin-1 mediates cell substrate adhesion and recruits Cdc42, Rac1, Pak1, and N-WASP into an intracellular signaling complex that promotes growth cone expansion. *J. Neurosci.* **25**, 3132-3141.
Souopgui, J., Sölter, M. and Pieler, T. (2002). XPak3 promotes cell cycle withdrawal during primary neurogenesis in Xenopus laevis. *EMBO J.* **21**, 6429-6439.
Sretavan, D. W. and Reichardt, L. F. (1993). Time-lapse video analysis of retinal ganglion cell axon pathfinding at the mammalian optic chiasm: growth cone guidance using intrinsic chiasm cues. *Neuron* **10**, 761-777.
Stofega, M. R., Sanders, L. C., Gardiner, E. M. and Bokoch, G. M. (2004). Constitutive p21-activated kinase (PAK) activation in breast cancer cells as a result of mislocalization of PAK to focal adhesions. *Mol. Biol. Cell* **15**, 2965-2977.
Tanaka, J., Yan, Y., Choi, J., Bai, J., Klenchin, V. A., Rayment, I. and Marriott, G. (2003). Biomolecular mimicry in the actin cytoskeleton: mechanisms underlying the cytotoxicity of kabiramide C and related macrolides. *Proc. Natl. Acad. Sci. USA* **100**, 13851-13856.
ten Klooster, J. P., Jaffer, Z. M., Chernoff, J. and Hordijk, P. L. (2006). Targeting and activation of Rac1 are mediated by the exchange factor beta-Pix. *J. Cell Biol.* **172**, 759-769.
Turner, C. E., Brown, M. C., Perrotta, J. A., Riedy, M. C., Nikolopoulos, S. N., McDonald, A. R., Bagrodia, S., Thomas, S. and Leventhal, P. S. (1999). Paxillin LD4 motif binds PAK and PIX through a novel 95-kD ankyrin repeat, ARF-GAP protein: A role in cytoskeletal remodeling. *J. Cell Biol.* **145**, 851-863.
Wiggan, O., Shaw, A. E., DeLuca, J. G. and Bamburg, J. R. (2012). ADF/cofilin regulates actomyosin assembly through competitive inhibition of myosin II binding to F-actin. *Dev. Cell* **22**, 530-543.
Woo, S. and Gomez, T. M. (2006). Rac1 and RhoA promote neurite outgrowth through formation and stabilization of growth cone point contacts. *J. Neurosci.* **26**, 1418-1428.
Woo, S., Rowan, D. J. and Gomez, T. M. (2009). Retinotopic mapping requires focal adhesion kinase-mediated regulation of growth cone adhesion. *J. Neurosci.* **29**, 13981-13991.
Wu, C., Asokan, S. B., Berginski, M. E., Haynes, E. M., Sharpless, N. E., Griffith, J. D., Gomez, S. M. and Bear, J. E. (2012). Arp2/3 is critical for lamellipodia and response to extracellular matrix cues but is dispensable for chemotaxis. *Cell* **148**, 973-987.
Zaidel-Bar, R. and Geiger, B. (2010). The switchable integrin adhesome. *J. Cell Sci.* **123**, 1385-1388.
Zaidel-Bar, R., Milo, R., Kam, Z. and Geiger, B. (2007). A paxillin tyrosine phosphorylation switch regulates the assembly and form of cell-matrix adhesions. *J. Cell Sci.* **120**, 137-148.
Zhang, H., Webb, D. J., Asmussen, H., Niu, S. and Horwitz, A. F. (2005). A GIT1/PIX/Rac/PAK signaling module regulates spine morphogenesis and synapse formation through MLC. *J. Neurosci.* **25**, 3379-3388.
Zhao, L., Ma, Q. L., Calon, F., Harris-White, M. E., Yang, F., Lim, G. P., Morihara, T., Ubeda, O. J., Ambegaokar, S., Hansen, J. E. et al. (2006). Role of p21-activated kinase pathway defects in the cognitive deficits of Alzheimer disease. *Nat. Neurosci.* **9**, 234-242.